

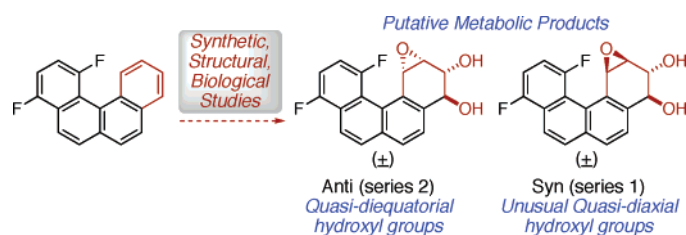
Synthetic, Crystallographic, Computational, and Biological Studies of 1,4-Difluorobenzo[*c*]phenanthrene and Its Metabolites

Suyeal Bae,^{†,‡} Heduck Mah,^{*,§} Surendrakumar Chaturvedi,^{||} Tamara Musafia Jeknic,[⊥] William M. Baird,[⊥] Amy K. Katz,[∇] H. L. Carrell,[∇] Jenny P. Glusker,[∇] Takao Okazaki,[○] Kenneth K. Laali,[○] Barbara Zajc,[‡] and Mahesh K. Lakshman^{*,‡}

Organic Chemistry Laboratory, Korea Institute of Science and Technology, P.O. Box 131, Cheongryang, Seoul 136-791, Korea, Department of Chemistry, Kyonggi University, Suwon 442-760, Korea, PrimeSyn Laboratories, Inc., 9 Ilene Court, Building 6, Units 1 and 2, Hillsborough, New Jersey 08844, Department of Environmental and Molecular Toxicology, Oregon State University, Corvallis, Oregon 97331, Fox Chase Cancer Center, 333 Cottman Avenue, Philadelphia, Pennsylvania 19111, Department of Chemistry, Kent State University, Kent, Ohio 44242, and Department of Chemistry, The City College and The City University of New York, 160 Convent Avenue, New York, New York 10031

lakshman@sci.ccny.cuny.edu

Received May 30, 2007



1,4-Difluorobenzo[*c*]phenanthrene (1,4-DFBcPh) and its putative metabolites, the dihydrodiol and diol epoxides, have been synthesized and structurally characterized, and the extent of DNA binding by the metabolites has been assessed. 1,4-DFBcPh and 1,4-difluoro-10-methoxybenzo[*c*]phenanthrene were prepared by photochemical cyclization of appropriate naphthylphenylethylenes. The dihydrodiol was synthesized from 1,4-difluoro-10-methoxybenzo[*c*]phenanthrene, and the diol epoxides were diastereoselectively synthesized from the dihydrodiol. Interesting differences were noted in ¹H NMR spectra of the series 1 (*syn*) diol epoxides of benzo[*c*]phenanthrene (BcPh) and 1,4-DFBcPh; the BcPh diol epoxide displays a quasi-diequatorial orientation of the hydroxyl groups, but in the 1,4-DFBcPh case these are diaxially disposed. This difference probably stems from the presence of the fjord-region fluorine atom in 1,4-DFBcPh. A through-space, fjord-region H–F coupling has also been observed for 1,4-DFBcPh and its derivatives. Comparative X-ray crystallographic analyses of BcPh and 1,4-DFBcPh and their dihydrodiols show that introduction of fluorine increases the molecular distortion by about 6–7°. As a guide to estimating the molecular distortion and its effects, and for comparison with the X-ray structures in known cases, optimized structures of BcPh, 1,4-DFBcPh, and 1,4-DMBcPh (the dimethyl analogue) as well as their dihydrodiols and diol epoxides were computed. Relative aromaticities of these compounds were assessed by nucleus-independent chemical shift calculations, and ¹³C NMR chemical shifts were computed by gauge-inducing atomic orbital calculations. 1,4-DFBcPh and its dihydrodiol were subjected to metabolism, and the amount of DNA binding in human breast cancer MCF-7 cells was assessed. The extent of DNA binding was then compared with that for BcPh and its dihydrodiol and the potent carcinogen benzo[*a*]pyrene. The 1,4-DFBcPh series 2 (*anti*) diol epoxide-derived DNA adducts were also compared with those arising from intracellular oxidation of the dihydrodiol with subsequent DNA binding. These experiments showed that increased molecular distortion decreased metabolic activation to the terminal metabolites but that diol epoxide metabolites that are formed are the DNA-damaging species.

Introduction

Among the diverse environmental pollutants produced by activities of a modern society, polycyclic aromatic hydrocarbons

(PAHs) are of particular interest because they present a health risk to humans. Metabolic activation of those PAHs that contain a bay or fjord region has been shown to proceed by the actions of cytochrome P450 and epoxide hydrolase. The result of this

* To whom correspondence should be addressed. Phone: (212) 650-7835. Fax: (212) 650-6107.

[†] Korea Institute of Science and Technology.

[‡] The City College and The City University of New York.

[§] Kyonggi University.

^{||} PrimeSyn Laboratories, Inc.

[⊥] Oregon State University (DNA binding).

[∇] Fox Chase Cancer Center (X-ray crystallography).

[○] Kent State University (computation).

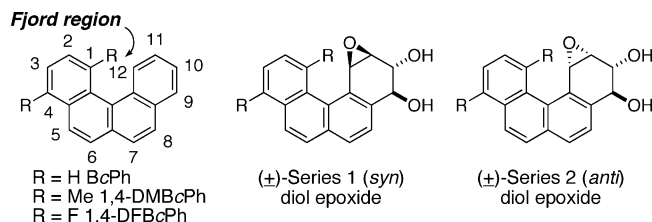


FIGURE 1. Structures of BcPh and its derivatives as well as their series 1 and series 2 diol epoxides.

metabolism is the formation of angular ring dihydrodiols (proximate carcinogens) and diol epoxides (ultimate carcinogens) that cause DNA damage, leading to mutations and the onset of tumorigenesis. Not only are dihydrodiols precursors to the diol epoxides,¹ but they can participate in dihydrodiol dehydrogenase-mediated redox cycling, producing reactive oxygen species and *o*-quinones, each of which can lead to DNA damage.^{2,3} Diol epoxides, on the other hand, are electrophiles that predominantly alkylate the purine bases in DNA via an S_N1-like epoxide ring opening process.⁴

Benzo[*c*]phenanthrene (BcPh) is the smallest PAH that contains a highly hindered fjord region (see Figure 1). It has been shown crystallographically that this compound is distorted from planarity by about 27°. Distortion in PAHs containing a highly hindered bay or fjord region leads to unusual properties. For example, in DNA alkylation nonplanar PAHs have been shown to produce a higher adenine/guanine adduct ratio as compared to planar ones.^{4b,c} In the case of the weakly carcinogenic BcPh,^{6,7} which is only poorly converted to the diol epoxide metabolites,⁸ the metabolites are highly potent and

exceptionally good DNA-alkylating agents.^{1c,9} Another interesting property resides in the conformational preferences of the BcPh diol epoxides (Figure 1). Normally it is found that the series 1 (*syn*) diol epoxides (*cis* arrangement of the benzylic hydroxyl group and oxirane) of bay region PAHs exhibit a quasi-diaxial arrangement of hydroxyl groups, whereas the series 2 (*anti*) isomers (*trans* arrangement of the benzylic hydroxyl and oxirane) exhibit a quasi-diequatorial arrangement.^{1c} However, both the series 1 and series 2 diol epoxides of BcPh have quasi-diequatorial hydroxyl groups.¹⁰ This may reflect steric overcrowding in the fjord region.

We have previously studied the influence of methylation on the BcPh system and have reported that the dimethyl derivative 1,4-DMBcPh (Figure 1) is distorted by about 37° from planarity.^{5a} This compound was found to be very poorly converted to diol epoxide metabolites and showed a significantly diminished extent of metabolism of its dihydrodiol to a diol epoxide in human breast cancer MCF-7 cells.^{5a} As a result of these findings we became interested in probing the influence of fluorine substitution on BcPh from the standpoint of its electronegativity as well as its ability to cause molecular distortion in the fjord region. We also wanted to investigate the efficiency of metabolism and the extent of DNA alkylation of the fluoro derivatives since the presence of fluorine can produce some unusual effects on the tumorigenic properties of PAHs. At comparable doses the 1-, 3-, 4-, and 6-fluoro derivatives of BcPh are marginally to significantly more potent than the parent hydrocarbon, whereas the 2-fluoro derivative has lower activity.⁷ On the basis of the increased potencies of 1- and 4-fluoro-BcPh, the difluoro compound 1,4-DFBcPh became an attractive target for our studies. This would allow direct comparisons of molecular distortion in relation to metabolism and DNA binding in a series of compounds, namely, BcPh, 1,4-DMBcPh, and 1,4-DFBcPh. In the present paper we describe the syntheses, three-dimensional structures (by X-ray crystallographic analyses and computational studies), metabolism, and DNA binding studies for 1,4-DFBcPh and some of its putative metabolites. The results are then compared with those for BcPh and 1,4-DMBcPh.

Results and Discussion

Synthesis of 1,4-DFBcPh and Its Diol Epoxide Metabolites.

Photochemical ring closure offers a convenient synthetic route to many angularly fused PAHs,^{11,12} and 1,4-DFBcPh has previously been prepared via such a route.^{13,14} Two possible alternatives were envisioned for the synthesis of 1,4-DFBcPh and a derivative with an oxidizable handle (Scheme 1). Route

(1) For reviews, please see: (a) *Polycyclic Aromatic Hydrocarbon Carcinogenesis: Structure-Activity Relationships*; Yang, S. K., Silverman, B. D., Eds.; CRC Press: Boca Raton, FL, 1988; Vols. I and II. *Polycyclic Aromatic Hydrocarbons: Chemistry and Carcinogenicity*; Harvey, R. G., Ed.; Cambridge University Press: Cambridge, U.K., 1991. (b) *Polycyclic Hydrocarbons and Carcinogenesis*; Harvey, R. G., Ed.; ACS Symposium Series 283; American Chemical Society: Washington, DC, 1985. (c) Jerina, D. M.; Sayer, J. M.; Agarwal, S. K.; Yagi, H.; Levin, W.; Wood, A. W.; Conney, A. H.; Pruess-Schwartz, D.; Baird, W. M.; Pigott, M. A.; Dipple, A. In *Biological Reactive Intermediates III*; Kocsis, J. J., Jollow, D. J., Witmer, C. M., Nelson, J. O., Snyder, R., Eds.; Plenum Press: New York, 1986; pp 11–30.

(2) For reviews, please see: (a) Bolton, J. L.; Trush, M. A.; Penning, T. M.; Dryhurst, G.; Monks, T. J. *Chem. Res. Toxicol.* **2000**, *13*, 135–160. (b) Penning, T. M.; Burczynski, M. E.; Hung, C.-F.; McCoull, K. D.; Palackal, N. T.; Tsuruda, L. S. *Chem. Res. Toxicol.* **1999**, *12*, 1–18.

(3) See, for example: (a) Park, J.-H.; Troxel, A. B.; Harvey, R. G.; Penning, T. M. *Chem. Res. Toxicol.* **2006**, *19*, 719–728. (b) Park, J.-H.; Gopishetty, S.; Szewczuk, L. M.; Troxel, A. B.; Harvey, R. G.; Penning, T. M. *Chem. Res. Toxicol.* **2005**, *18*, 1026–1037. (c) Yu, D.; Berlin, J. A.; Penning, T. M.; Field, J. *Chem. Res. Toxicol.* **2002**, *15*, 832–842. (d) McCoull, K. D.; Rindgen, D.; Blair, I. A.; Penning, T. M. *Chem. Res. Toxicol.* **1999**, *12*, 237–246.

(4) (a) Melendez-Colon, V. J.; Luch, A.; Seidel, A.; Baird, W. M. *Carcinogenesis* **1999**, *20*, 1885–1891. (b) Szeliga, J.; Dipple, A. *Chem. Res. Toxicol.* **1998**, *11*, 1–11. (c) Dipple, A. In *DNA Adducts: Identification and Biological Significance*; Hemminki, K., Dipple, A., Shuker, D. E. G., Kadlubar, F. F., Sagerbäck, D.; Bartsch, H., Eds.; Scientific Publication No. 125; International Agency for Research on Cancer: Lyon, France, 1994; pp 107–129. (d) Jerina, D. M.; Chadha, A.; Cheh, A. M.; Schurdak, M. E.; Wood, A. W.; Sayer, J. M. In *Biological Reactive Intermediates IV*; Witmer, C. M., Snyder, R., Jollow, D. J., Kalf, G. F., Kocsis, J. J., Sipes, I. G., Eds.; Plenum Press: New York, 1991; pp 533–553.

(5) (a) Lakshman, M. K.; Kole, P.; Chaturvedi, S.; Saugier, J. H.; Yeh, H. J. C.; Glusker, J. P.; Carrell, H. L.; Katz, A. K.; Afshar, C. E.; Dashwood, W.-M.; Kenniston, G.; Baird, W. M. *J. Am. Chem. Soc.* **2000**, *122*, 12629–12636. (b) Hirshfeld, F. L.; Sandler, S.; Schmidt, G. M. J. *J. Chem. Soc.* **1963**, 2108–2125.

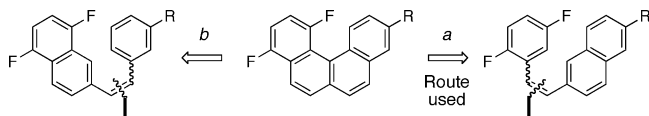
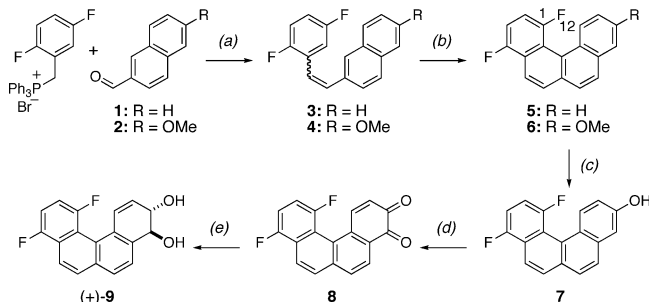
(6) Levin, W.; Wood, A. W.; Chang, R. L.; Ittah, Y.; Croisy-Delcey, M.; Yagi, H.; Jerina, D. M.; Conney, A. H. *Cancer Res.* **1980**, *40*, 3910–3914.

(7) Jerina, D. M.; Sayer, J. M.; Yagi, H.; Croisy-Delcey, M.; Ittah, Y.; Thakker, D. R.; Wood, A. W.; Chang, R. L.; Levin, W.; Conney, A. H. In *Biological Reactive Intermediates II Part A*; Snyder, R., Parke, D. V., Kocsis, J. J., Jollow, D. J., Gibson, C. G., Witmer, C. M., Eds.; Plenum Press: New York, 1982; pp 501–523.

(8) (a) Thakker, D. R.; Levin, W.; Yagi, H.; Herman, H. J. C.; Ryan, D. E.; Thomas, P. E.; Conney, A. H.; Jerina, D. M. *J. Biol. Chem.* **1986**, *261*, 5404–5413. (b) Ittah, Y.; Thakker, D. R.; Levin, W.; Croisy-Delcey, M.; Ryan, D. E.; Thomas, P. E.; Conney, A. H.; Jerina, D. M. *Chem.-Biol. Interact.* **1983**, *45*, 15–28.

(9) Agarwal, S. K.; Sayer, J. M.; Yeh, H. J. C.; Pannell, L. K.; Hilton, B. D.; Pigott, M. A.; Dipple, A.; Yagi, H.; Jerina, D. M. *J. Am. Chem. Soc.* **1987**, *109*, 2497–2504.

(10) Sayer, J. M.; Yagi, H.; Croisy-Delcey, M.; Jerina, D. M. *J. Am. Chem. Soc.* **1981**, *103*, 4970–4972.

SCHEME 1. Two Possible Retrosyntheses of 1,4-DFBcPh and a Derivative Suitable for Further Manipulation**SCHEME 2. Synthesis of 1,4-DFBcPh and Its Dihydrodiol^a**

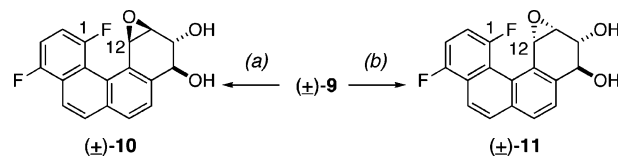
^a Reagents and conditions: (a) NaOMe, MeOH, rt; (b) PhH, I₂, air, *hν*; (c) BBr₃, CH₂Cl₂, 0 °C to rt; (d) (PhSeO)₂O, THF, reflux; (e) NaBH₄, EtOH, O₂, rt.

a would involve a photocyclization of (2,5-difluorophenyl)-naphthylethene, whereas route b would involve a similar cyclization of a (difluoronaphthyl)phenylethene (R = a substituent that can be used for elaboration to the oxidized metabolites).

In comparing the two approaches, route b would require construction of a 6-substituted 1,4-difluoronaphthalene, but route a would simply involve a Wittig reaction between a difluorophenyl derivative and a suitable 2,6-disubstituted naphthalene. This, combined with the commercial availability of 2-naphthaldehyde, 6-methoxy-2-naphthaldehyde, and 2,5-difluorobenzyl bromide led us to pursue route a.

2,5-Difluorobenzyl bromide was converted to its known phosphonium salt by reaction with PPh₃ in toluene at reflux.^{5a,14} Wittig reaction between this phosphonium salt and 2-naphthaldehyde yielded a ~1:2 mixture of the known alkenes **3**^{13,14} (Scheme 2). Photochemical ring closure of this alkene mixture **3** in a Hanovia reactor using a 450 W medium-pressure Hg lamp with catalytic I₂ and air yielded 1,4-DFBcPh (**5**) (64%).^{13,14} Comparable yields (71%^{13,14}) have been reported under the Katz conditions.¹⁵

With **5** synthesized, attention was directed to the synthesis of its putative metabolites. Again, a Wittig reaction between the phosphonium salt derived from (2,5-difluorobenzyl)triphenylphosphonium bromide and 6-methoxy-2-naphthaldehyde yielded the methoxy-substituted alkene mixture **4** (~1:3 ratio, 70%). Photochemical ring closure of **4** as described above

SCHEME 3. Synthesis of the Series 1 (*syn*) and Series 2 (*anti*) Diol Epoxides^a

^a Reagents and conditions: (a) (i) *N*-bromoacetamide, THF–H₂O, rt; (ii) Amberlite HO[−], THF, rt; (b) *m*-CPBA, THF, rt.

afforded 1,4-difluoro-10-methoxy-BcPh (**6**) in 58% yield. Cleavage of the methoxy group in **6** was accomplished with BBr₃ in CH₂Cl₂ (88%), and the ensuing phenol **7** was oxidized to the *o*-quinone **8** with benzeneselenic anhydride in THF (87%).^{5a} Finally, reduction of the *o*-quinone **8** with NaBH₄ in EtOH under O₂ sparge¹⁶ provided the racemic dihydrodiol **9** in 79% yield.

With (±)-**9** at hand, subsequent steps were its conversion to the series 1 and series 2 diol epoxides. As determined by ¹H NMR, (±)-**9** exhibits a diequatorial arrangement of the hydroxyl groups, indicating that the presence of fluorine did not produce any unusual conformational changes at this stage. Therefore, on the basis of prior literature precedent,¹⁷ it was anticipated that a single bromo triol could be obtained by reaction of (±)-**9** with *N*-bromoacetamide in wet THF. This was indeed the case, and cyclization of the bromo triol with dry Amberlite resin in anhydrous THF yielded series 1 diol epoxide (±)-**10** (Scheme 3, two steps, 68% yield). On the basis of a similar literature precedent,¹⁷ reaction of (±)-**9** with *m*-CPBA yielded the series 2 diol epoxide diastereomer (±)-**11** (92% yield, Scheme 3).

¹H and ¹⁹F NMR Characteristics of the 1,4-DFBcPh Derivatives. BcPh derivatives **5–9** exhibit an interesting feature in their NMR spectra; the proton in the fjord region displays coupling to the fjord-region fluorine. This is clearly discernible in the ¹H NMR spectra of **6** and **7** where the most downfield aromatic proton shows a dd pattern with $J_{\text{H,F}} \approx 14$ Hz. In *o*-quinone **8** the most downfield quinonoid vinyl proton (residing in the fjord region) appears as a doublet of doublets at δ 7.83 ppm with $J_{\text{H,H}} = 10.6$ Hz and $J_{\text{H,F}} = 15.6$ Hz. In contrast, the comparable vinyl proton in the unfluorinated BcPh *o*-quinone appears as a doublet with $J_{\text{H,H}} = 10.5$ Hz. Finally, in dihydrodiol **9** the fjord-region vinyl proton appears as a doublet of doublets of doublets with $J_{\text{H,H}} = 10.2$ and 2.2 Hz and $J_{\text{H,F}} = 15.6$ Hz.

The diol epoxides again display coupling between the proton and fluorine in the fjord region. In the case of (±)-**10**, $J_{\text{H,F}} = 10.8$ Hz, whereas in (±)-**11**, $J_{\text{H,F}} = 11.2$ Hz. These H–F coupling constants are smaller than those observed in the completely aromatic or vinyl systems in Scheme 2. On the basis of the fact that the fjord-region proton in the diol epoxides no longer resides on an sp² carbon, we believe that the origin of proton–fluorine coupling observed in each of these cases is spatial proximity of these nuclei.

In the ¹⁹F NMR spectra of compounds **5–11** the more upfield non-fjord-region fluorine consistently appears as a sharp ddd representing one F–F coupling and two F–H couplings. On the other hand, the downfield fjord-region fluorine shows a more complex pattern appearing as a broadened doublet of multiplets in **5**, **6**, **8**, and **9**, a broadened multiplet in **7** and (±)-**10**, or a

(11) (a) Mallory, F. B.; Rudolph, M. J.; Oh, S. M. *J. Org. Chem.* **1989**, *54*, 4619–4626. (b) Mallory, F. B.; Mallory, C. W. *J. Am. Chem. Soc.* **1972**, *94*, 6041–6048. (c) Mallory, F. B.; Gordon, J. T.; Wood, C. S. *J. Am. Chem. Soc.* **1963**, *85*, 828–829. (d) Mallory, F. B.; Wood, C. S.; Gordon, J. T.; Lindquist, L. C.; Savitz, M. L. *J. Am. Chem. Soc.* **1962**, *84*, 4361–4362.

(12) (a) Misra, B.; Amin, S. *J. Org. Chem.* **1990**, *55*, 4478–4480. (b) Amin, S.; Camanzo, J.; Huie, K.; Hecht, S. S. *J. Org. Chem.* **1984**, *49*, 381–384. (c) Utermohlen, C. M.; Singh, M.; Lehr, R. E. *J. Org. Chem.* **1987**, *52*, 5574–5582. (d) Amin, S.; Hecht, S. S.; LaVoie, E.; Hoffmann, D. *J. Med. Chem.* **1979**, *22*, 1336–1340.

(13) Plater, J. M. *Tetrahedron Lett.* **1994**, *35*, 6147–6150.

(14) Plater, J. M. *J. Chem. Soc., Perkin Trans. 1* **1997**, 2903–2909.

(15) Liu, L.; Yang, B.; Katz, T. J.; Poindexter, M. K. *J. Org. Chem.* **1991**, *56*, 3769–3775.

(16) Platt, K. L.; Oesch, F. *J. Org. Chem.* **1983**, *48*, 265–268.

(17) Yagi, H.; Thakker, D. R.; Hernandez, O.; Koreeda, M.; Jerina, D. M. *J. Am. Chem. Soc.* **1977**, *99*, 1604–1611.

very broad signal in (\pm)-**11**. All of these results are again indicative of a through-space F–H coupling. This phenomenon (which consistently appears in many of the derivatives described here) has not been reported previously for 1,4-DFBcPh,^{13,14} but it has been documented for several fluorohydrocarbons¹⁸ including 1-fluoro-BcPh derivatives.¹⁹ The H–F coupling constants observed here are quite large, in the range of 14–15 Hz when the F atom is at an sp² carbon, and are comparable to reported values.¹⁹ This F–H coupling across the fjord region is likely related to nonbonded overlap of F1 and H12.¹⁹ From the X-ray crystallographic analysis (described later) the internuclear distances between the fluorine and hydrogen atoms on either side of the fjord region are 2.2(1) and 2.3(1) Å in **5** and (\pm)-**9**, respectively. By comparison, the internuclear distances between the hydrogen atoms on either side of the fjord region in BcPh and its dihydrodiol are 1.9(1) and 2.1(1) Å, respectively. In 1,4-DMBcPh the internuclear distance between the fjord-region methyl hydrogen and the hydrogen atom on the other side of the fjord region is 2.1(1) Å.

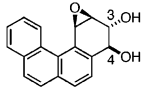
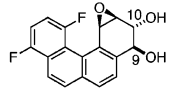
Conformations of the BcPh and 1,4-DFBcPh Diol Epoxides. The ¹H NMR results also provide an understanding of the conformational preferences of the hydroxyl groups in the diol epoxides. The series 2 (*anti*) diol epoxides of BcPh and 1,4-DFBcPh have a comparable diequatorial arrangement of the hydroxyl groups ($J_{3,4} = 8.3$ Hz and $J_{9,10} = 8.5$ Hz, respectively, in DMSO-*d*₆). In contrast, a curious feature emerges when the ¹H NMR data of the series 1 (*syn*) diol epoxides of BcPh and 1,4-DFBcPh are compared. The series 1 BcPh diol epoxide (the first such compound to display a quasi-diequatorial arrangement of the hydroxyl groups) has $J_{3,4} = 9.0$ Hz (in DMSO-*d*₆) between H₃ and H₄.¹⁰ Reanalysis of the coupling constant of this diol epoxide in the present study using acetone-*d*₆ confirmed this value. However, $J_{9,10}$ of the 1,4-DFBcPh series 1 diol epoxide was a much smaller 2.1 Hz (acetone-*d*₆), indicating a quasi-diaxial arrangement of the hydroxyl groups in this case. On the other hand, this 1,4-DFBcPh diol epoxide displayed a much larger coupling between the benzylic H₉ proton and the benzylic hydroxyl proton OH₉ than did the nonfluorinated analogue (Table 1). This coupling constant is due to a large dihedral angle between OH₉ and H₉ that is probably a result of intramolecular hydrogen bonding between the OH₉ proton and the epoxide oxygen. Such a hydrogen bond would be consistent with a diaxial arrangement of the hydroxyls, which is reflected in the much smaller $J_{9,10}$ in the 1,4-DFBcPh case. Thus, it appears that either the presence of the fluorine in the fjord region or the additional molecular distortion may be the origin of this unexpected conformational shift in the difluoro analogue.

X-ray Crystallographic Analysis of 1,4-DFBcPh (5**) and Its Dihydrodiol **9**.** We have previously reported the X-ray crystallographic analysis of BcPh and 1,4-DMBcPh, wherein addition of methyl groups at positions 1 and 4 in the BcPh skeleton was shown to increase the nonplanarity by 10°, mainly because of steric overcrowding in the fjord region.^{5a} Using

(18) (a) Krccmar, L.; Grunenberg, J.; Dix, I.; Jones, P. G.; Ibrom, K.; Ernst, L. *Eur. J. Org. Chem.* **2005**, 5306–5312. (b) Yamamoto, G.; Oki, M. *J. Org. Chem.* **1984**, *49*, 1913–1917. (c) Mallory, F. B.; Mallory, C. W.; Ricker, W. M. *J. Am. Chem. Soc.* **1975**, *97*, 4770–4771. (d) Abushanab, E. *J. Am. Chem. Soc.* **1971**, *93*, 6532–6536. (e) Gribble, G. W.; Douglas, J. R., Jr. *J. Am. Chem. Soc.* **1970**, *92*, 5764–5765. (f) Jefford, C. W.; Hill, D. T.; Ghosez, L.; Toppet, S.; Ramey, K. C. *J. Am. Chem. Soc.* **1969**, *91*, 1532–1534. (g) Myhre, P. C.; Edmonds, J. W.; Kruger, J. D. *J. Am. Chem. Soc.* **1966**, *88*, 2459–2466.

(19) Mallory, F. B.; Mallory, C. W.; Ricker, W. M. *J. Org. Chem.* **1985**, *50*, 457–461.

TABLE 1. CH–OH Coupling Constants (Hz) in BcPh and 1,4-DFBcPh Series 1 (*syn*) Diol Epoxides

solvent				
	J_{H3-OH3}	J_{H4-OH4}	$J_{H10-OH10}$	J_{H9-OH9}
CDCl ₃	5.4	8.3	8.0	12.1
THF- <i>d</i> ₈	4.4	5.9	5.8	11.7
Acetone- <i>d</i> ₆	4.4	6.3	6.1	11.6
DMSO- <i>d</i> ₆	4.9	6.3	5.1	8.0

MCF-7 human carcinoma cells, we also showed that 1,4-DMBcPh exhibited 3-fold-lower DNA damage as compared to BcPh, which was itself only poorly metabolized.^{5a} This was attributed, at least in part, to increased distortion in 1,4-DMBcPh that could influence its metabolic activation. To continue the understanding of structure in relation to metabolic activation, we have succeeded in acquiring crystallographic data on the BcPh dihydrodiol and 1,4-DFBcPh and its dihydrodiol. These data are presented in Table 2 as angles between the four planes (A–D) of the compounds. Previously reported data on BcPh and 1,4-DMBcPh^{5a} are also included in this table for comparison.

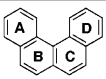
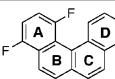
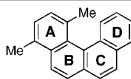
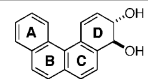
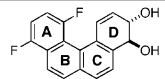
The most obvious feature that emerges from Table 2 is the angle between the A and D planes that represents the overall molecular distortion. Although the methyl groups dramatically increase nonplanarity of the BcPh skeleton by about 10°, the fluorine atoms also produce a large distortion by nearly 7° in 1,4-DFBcPh. Across the three parent hydrocarbons, the trend is that the angles between the planes increase from left to right. Another curious feature comes to light when the interplane angles for BcPh and 1,4-DFBcPh and their dihydrodiols are compared. In each case, the overall molecular distortion (shown by the B–D and A–D interplane angles) is diminished upon oxidation of the D ring (see Table 2 as well as Table 3 for data on 1,4-DMBcPh and its dihydrodiol). These crystallographic results (also see Figure 2) may be useful when the DNA adducts resulting from the diol epoxides of such hydrocarbons are studied.

Computational Analyses of the PAH Metabolites. Parent BcPh, 1,4-DMBcPh, and 1,4-DFBcPh (**5**) and the corresponding

(20) Frisch, M. J.; Trucks, G. W.; Schlegel, H. B.; Scuseria, G. E.; Robb, M. A.; Cheeseman, J. R.; Montgomery, J. A., Jr.; Vreven, T.; Kudin, K. N.; Burant, J. C.; Millam, J. M.; Iyengar, S. S.; Tomasi, J.; Barone, V.; Mennucci, B.; Cossi, M.; Scalmani, G.; Rega, N.; Petersson, G. A.; Nakatsuji, H.; Hada, M.; Ehara, M.; Toyota, K.; Fukuda, R.; Hasegawa, J.; Ishida, M.; Nakajima, T.; Honda, Y.; Kitao, O.; Nakai, H.; Klene, M.; Li, X.; Knox, J. E.; Hratchian, H. P.; Cross, J. B.; Adamo, C.; Jaramillo, J.; Gomperts, R.; Stratmann, R. E.; Yazyev, O.; Austin, A. J.; Cammi, R.; Pomelli, C.; Ochterski, J. W.; Ayala, P. Y.; Morokuma, K.; Voth, G. A.; Salvador, P.; Dannenberg, J. J.; Zakrzewski, V. G.; Dapprich, S.; Daniels, A. D.; Strain, M. C.; Farkas, O.; Malick, D. K.; Rabuck, A. D.; Raghavachari, K.; Foresman, J. B.; Ortiz, J. V.; Cui, Q.; Baboul, A. G.; Clifford, S.; Cioslowski, J.; Stefanov, B. B.; Liu, G.; Liashenko, A.; Piskorz, P.; Komaromi, I.; Martin, R. L.; Fox, D. J.; Keith, T.; Al-Laham, M. A.; Peng, C. Y.; Nanayakkara, A.; Challacombe, M.; Gill, P. M. W.; Johnson, B.; Chen, W.; Wong, M. W.; Gonzalez, C.; Pople, J. A. *Gaussian 03*, Revision B.05; Gaussian, Inc.: Pittsburgh, PA, 2003.

(21) Wolfram, K.; Holthausen, M. C. *A Chemist's Guide to Density Functional Theory*, 2nd ed.; Wiley-VCH: Weinheim, Germany, 2000.

TABLE 2. Angles between the Four Planes of BcPh^{5a} and Its Derivatives Determined Crystallographically

angle between					
A, B	10.3°	12.0°	12.4°	10.2°	13.3°
A, C	18.1°	23.6°	25.0°	17.9°	23.5°
B, C	7.9°	11.9°	13.1°	9.2°	10.7°
B, D	16.6°	21.7°	24.7°	6.7°	9.1°
C, D	8.8°	10.2°	11.7°	8.0°	6.2°
A, D	26.7°	33.5°	36.6°	16.3°	22.4°
estimated error e.s.d	0.1°	0.1°	0.1°	0.2°	0.3°

dihydrodiols and their series 2 and series 1 diol epoxides were studied by density functional theory (DFT) with Becke's three-parameter and Lee–Yang–Parr correlation function and a medium-sized basis set, B3LYP/6-31G(d) level, which have evolved as a standard tool.^{20,21} For the dihydrodiols, four conformations had minimum energies; they consisted of two quasi-diaxial and quasi-diequatorial pairs, existing as the a-form and b-form (Figure 3 and Table 1 in the Supporting Information). The quasi-diequatorial conformations (in the a-form) were preferred for all three dihydrodiols, with the quasi-diaxial conformations being on average about 2 kcal/mol higher in energy. The computationally inferred preference for the quasi-diequatorial conformation in the dihydrodiols agreed with the NMR-based conclusions reported here and previously.

For the series 1 and series 2 diol epoxides four conformations (for each series) were found to be minima, consisting of two quasi-diaxial and quasi-diequatorial pairs (see Table 1 in the Supporting Information). For series 1 diol epoxides, in the case of BcPh the quasi-diaxial/quasi-diequatorial conformations are both preferred in the gas phase and have nearly the same energy, whereas for those of 1,4-DFBcPh and 1,4-DMBcPh the quasi-diaxial conformations are clearly preferred for both, and this is in agreement with the NMR-based conclusions. For the series 2 diol epoxides, the quasi-diequatorial orientations (b-*anti*-in form) were preferred over the alternatives, and these findings are also in accord with the solution conformations. Although with the series 2 diol epoxide of BcPh the difference between the lowest energy diaxial/diequatorial forms was only 0.5 kcal/mol, the energy difference was greater in the case of 1,4-disubstituted derivatives.

Comparison of the Computational Data with the X-ray Results. Table 3 summarizes the computed angles between the four planes of BcPh and its derivatives and provides a comparison with the X-ray-derived data. To examine the influence of the method and the basis set on the computed values, BcPh and 1,4-DFBcPh and their dihydrodiols as well as 1,4-DMBcPh were reoptimized by the DFT method with larger basis sets, B3LYP/6-31+G(d,p) and B3LYP/6-311+G(2d,p), Hartree–Fock method, HF/6-31+G(d,p), and second-order Moller–Plesset perturbation theory method, MP2/3-21G. The Hartree–Fock method includes poor electron correlation. MP2 treats the electron correlation correction by the ab initio method and demands much greater computational

resources. It can be seen that the correspondence is generally good and that B3LYP/6-31G(d) appears adequate, since differences between the X-ray data and the calculated values do not seem to narrow further by augmenting the basis set. The optimized structures for the 12 compounds calculated by B3LYP/6-31G(d) are shown in Figure 1 of the Supporting Information.

Some Comparisons of Computational, X-ray, and NMR Data. In the context of the present study and as a guide to experimental NMR studies, carbon and fluorine NMR data were computed for these compounds by the gauge-inducing atomic orbital (GIAO) method,²² which computes the magnetic shielding tensor for nuclei (see Figure 2 in the Supporting Information). These results show that the aromatic ring carbons fall into a fairly narrow chemical shift range. In the dihydrodiol and the diol epoxides the A/B ring junction α to hydroxyl is most deshielded. The helical structure of the methylated derivatives leads to nonequivalence of the methyl groups, and the existence of atropisomerism in 1,4-DMBcPh has previously been observed by NMR.^{5a} Relative downfield shifts of the methyl and the fluorine substituents in the fjord region due to the buttressing effect are nicely predicted by GIAO and are in line with expectation.


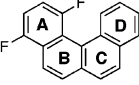
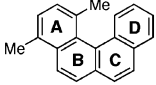
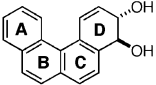
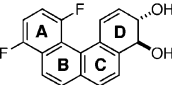
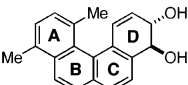
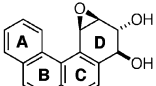
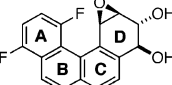
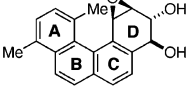
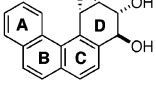
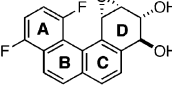
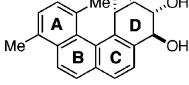
Since the experimental findings demonstrated a through-space F–H coupling across the fjord region in 1,4-DFBcPh and its derivatives, the F–H bond distances were computed by B3LYP/6-31G(d). Table 4 summarizes the computational and crystallographic results together with the observed F–H coupling constants and distances from the optimized structures.

Finally, to gain some insight into the relative aromaticity in various rings in BcPh derivatives described here, the GIAO-derived nucleus-independent chemical shift (NICS) values,²³ which are known as computed aromaticity indexes, were computed (Figure 3 of the Supporting Information). In the parent BcPh, 1,4-DFBcPh, and 1,4-DMBcPh the angular (A and D) rings are most aromatic, and the relative aromaticity in the B ring in 1,4-DFBcPh and 1,4-DMBcPh is somewhat diminished. These features are consistent with out-of-plane twisting and loss

(22) (a) Wolinski, K.; Hinton, J. F.; Pulay, P. *J. Am. Chem. Soc.* **1990**, *112*, 8251–8260. (b) Ditchfield, R. *Mol. Phys.* **1974**, *27*, 789–807.

(23) Schleyer, P. v. R.; Maerker, C.; Dransfeld, A.; Jiao, H.; Hommes, N. J. v. E. *J. Am. Chem. Soc.* **1996**, *118*, 6317–6318.

TABLE 3. Computed Angles (deg) between the Average Planes of the Aromatic Rings in BcPh and Its Derivatives and Comparison to X-ray Data^a

compound	method	A, B	A, C	A, D	B, C	B, D	C, D
	X-ray	10.3	18.1	26.7	7.9	16.6	8.8
	B3LYP/6-31G(d)	9.4	18.4	27.8	9.0	18.4	9.4
	B3LYP/6-31+G(d,p)	8.0	20.5	28.5	12.5	20.5	8.0
	B3LYP/6-311+G(2d,p)	8.1	20.6	28.7	12.5	20.6	8.1
	HF/6-31+G(d,p)	9.8	19.0	28.8	9.2	19.0	9.8
	MP2/3-21G	10.7	20.2	30.8	9.5	20.2	10.7
	X-ray	12.0	23.6	33.5	11.9	21.7	10.2
	B3LYP/6-31G(d)	11.5	22.6	33.5	11.1	21.9	10.9
	B3LYP/6-31+G(d,p)	11.8	23.2	34.1	11.5	22.3	10.9
	B3LYP/6-311+G(2d,p)	12.0	23.5	34.7	11.7	22.8	11.2
	HF/6-31+G(d,p)	12.0	23.6	34.9	11.7	22.9	11.3
	MP2/3-21G	11.8	23.0	35.1	11.4	23.3	12.0
	X-ray	12.4	25.0	36.6	13.1	24.7	11.7
	B3LYP/6-31G(d)	14.0	27.6	39.5	13.7	25.5	12.2
	B3LYP/6-31+G(d,p)	14.2	28.0	39.8	13.9	25.6	12.2
	B3LYP/6-311+G(2d,p)	14.3	28.2	40.1	13.9	25.8	12.3
	HF/6-31+G(d,p)	14.4	28.4	40.3	14.1	25.9	12.3
	MP2/3-21G	14.1	27.5	40.1	13.5	26.0	13.0
	X-ray	10.2	17.9	16.3	9.2	6.7	8.0
	B3LYP/6-31G(d)	8.7	16.0	16.5	7.4	9.8	9.1
	B3LYP/6-31+G(d,p)	8.9	16.2	17.6	7.4	10.3	8.6
	B3LYP/6-311+G(2d,p)	9.0	16.4	17.6	7.5	10.1	8.6
	HF/6-31+G(d,p)	9.2	16.6	17.9	7.5	10.3	8.9
	MP2/3-21G	9.8	17.2	17.0	7.6	9.7	10.7
	X-ray	13.3	23.5	22.4	10.7	9.1	6.2
	B3LYP/6-31G(d)	11.7	21.9	22.0	10.6	10.5	7.2
	B3LYP/6-31+G(d,p)	11.8	22.3	23.2	10.8	11.6	6.9
	B3LYP/6-311+G(2d,p)	12.0	22.7	23.5	11.1	11.6	6.8
	HF/6-31+G(d,p)	12.2	22.7	23.6	11.0	11.6	7.0
	MP2/3-21G	11.9	22.1	21.0	11.1	9.2	8.2
	B3LYP/6-31G(d)	14.0	26.8	29.6	13.1	15.6	6.5
		B3LYP/6-31G(d)	9.5	17.8	37.4	8.3	28.1
	B3LYP/6-31G(d)	12.0	22.4	45.2	10.7	33.7	23.0
		B3LYP/6-31G(d)	14.3	27.8	52.2	13.9	38.1
	B3LYP/6-31G(d)	9.9	18.7	37.0	8.9	27.5	18.9
	B3LYP/6-31G(d)	12.5	23.2	46.9	10.8	35.1	24.7
	B3LYP/6-31G(d)	18.9	30.4	56.5	11.6	37.6	26.0

^a Average planes of the aromatic rings were estimated by a least-squares method.

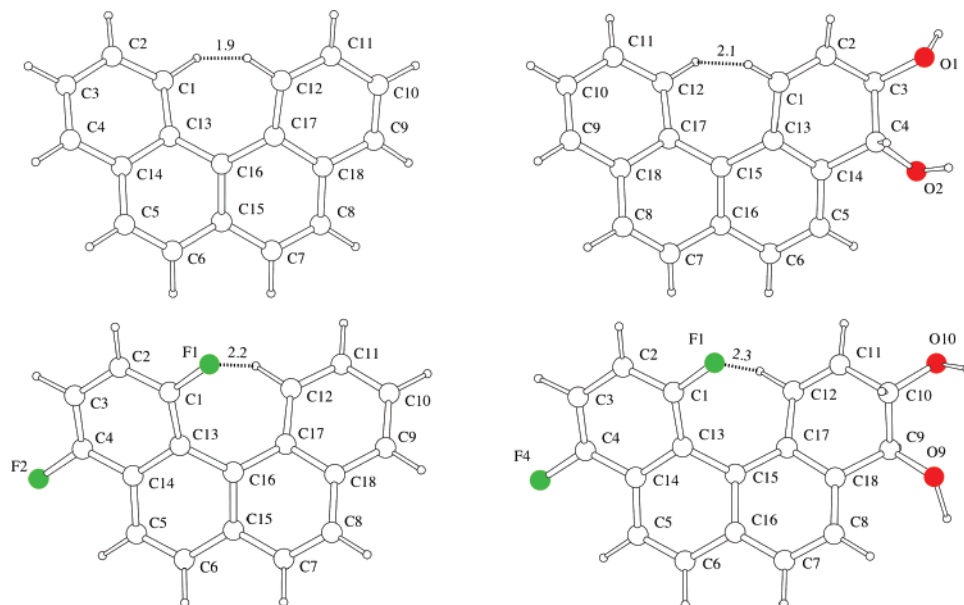


FIGURE 2. Structures of BcPh^{5a} and its dihydrodiol (top row) and 1,4-DFBcPh and its dihydrodiol (bottom row) determined by X-ray crystallographic analysis.

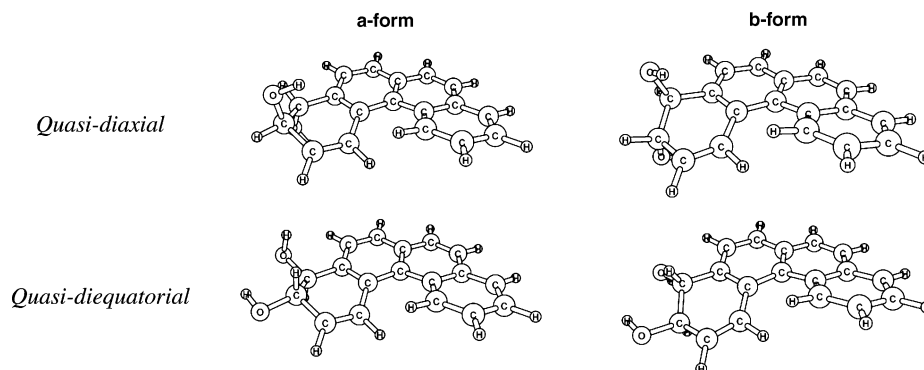


FIGURE 3. Four conformations of the BcPh dihydrodiol.

TABLE 4. Computed and Crystallographically Determined F–H Bond Distances (Å) as Well as Observed Coupling Constants

compd	calcd F–H distance	F–H distance by X-ray	$J_{F,H}$ (Hz)
5	2.232	2.20(1)	15.5 (CDCl ₃) 15.1 (C ₆ D ₆)
(±)- 9	2.370	2.36(1)	15.4 (CDCl ₃) 15.6 (DMSO- <i>d</i> ₆)
(±)- 10	2.298		10.8 (acetone- <i>d</i> ₆)
(±)- 11	2.299		11.2 (acetone- <i>d</i> ₆)

of conjugation. Relative aromaticity in the C ring increases in the dihydrodiol and diol epoxides as compared to the hydrocarbon precursors.

Metabolism and DNA Binding of the PAHs and Their Dihydrodiols. Human mammary (gland) carcinoma cell line MCF-7 was treated for 24 h with benzo[*a*]pyrene (BaP; positive control), DMSO (negative control), and each of the benzo[*c*]phenanthrene derivatives BcPh, 1,4-DFBcPh, and 1,4-DMBcPh and their dihydrodiols. The extent of DNA damage in each case was measured by ³³P postlabeling of the DNA and HPLC analysis of the DNA adducts produced. The results of these experiments are summarized in Table 5.

TABLE 5. Extent of DNA Damage Determined by ³³P Postlabeling

compd	DNA adduct levels (pmol of adduct/mg of DNA)		
	no. of samples ^a	av	std dev
DMSO	4	0	0
BaP (4 μM)	10	32 ^b	27.2
BcPh (5 μM)	8	0 ^c	0
BcPh dihydrodiol (1 μM)	8	7.8 ^d	5.9
1,4-DFBcPh (5 μM)	8	0	0
1,4-DFBcPh dihydrodiol (1 μM)	10	2.0 ^e	2.5
1,4-DMBcPh (5 μM)	7	0	0
1,4-DMBcPh dihydrodiol (1 μM)	9	0	0

^a The number of samples represents the number of independent samples, each from one separate cell treatment. ^{b–e} Significantly different from each other at the 5% level on the basis of one-way ANOVA (analysis of variance).

For internal consistency, all compounds were tested concurrently. BcPh, 1,4-DFBcPh, and 1,4-DMBcPh did not undergo significant metabolic activation (we have previously reported very low levels of activation of BcPh and 1,4-DMBcPh^{5a}). In contrast, the dihydrodiols of BcPh and 1,4-DFBcPh underwent metabolic activation to DNA-damaging agents, and 1,4-DFBcPh dihydrodiol produced significantly fewer DNA adducts.

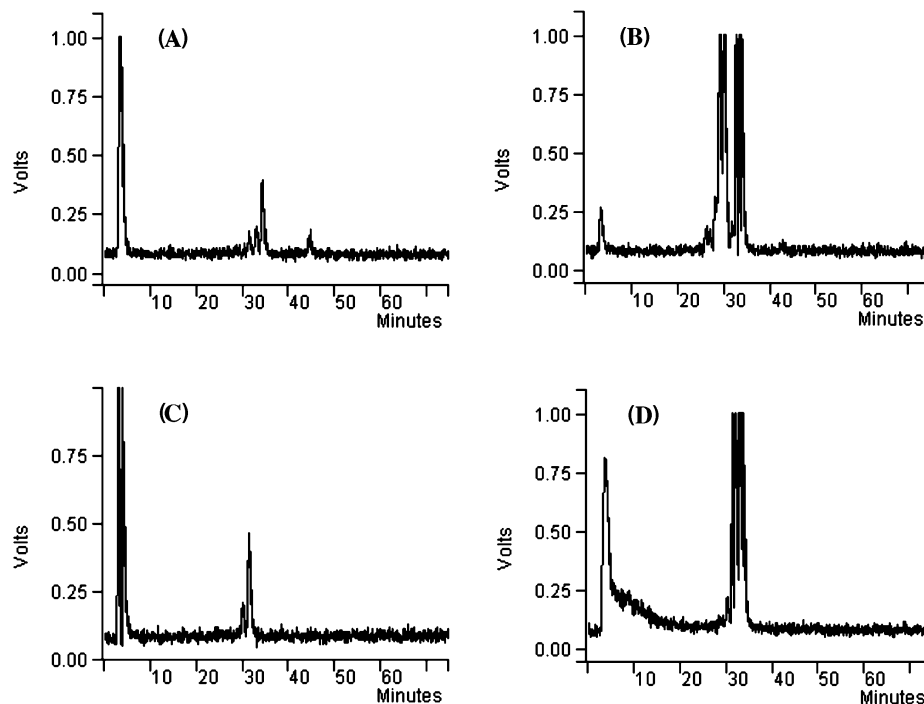


FIGURE 4. HPLC profiles of DNA adducts derived by incubation of (A) BcPh, (B) BcPh diol epoxide, (C) 1,4-DFBcPh, and (D) 1,4-DFBcPh diol epoxide with MCF-7 cells (1 V contained 5000 disintegrations per minute).

In our previous work on 1,4-DMBcPh and its metabolites we had proposed the idea that metabolic activation could depend on the overall molecular distortion.^{5a} In that study a 3-fold-lower metabolic activation of 1,4-DMBcPh occurred in comparison to that of BcPh, whereas activation of 1,4-DMBcPh dihydrodiol to DNA-damaging agents was 11-fold lower than that of BcPh dihydrodiol. This suggested the possibility that increased distortion influences the final oxidation of the dihydrodiol to the DNA-damaging diol epoxide. Consistent with this notion, 1,4-DFBcPh dihydrodiol showed an approximately 4-fold-lowered activation than the BcPh dihydrodiol. Thus, molecular nonplanarity does seem to have a role in the metabolic activation process, with increasing nonplanarity resulting in attenuation. In line with our previous studies,^{5a} it appears that the final oxidation of the dihydrodiol at the fjord region may be more prone to diminished metabolism as a result of the molecular distortion and/or steric effects.

Subsequently, we also wanted to determine whether diol epoxides resulting from metabolic activation of the dihydrodiols are the ultimate DNA-damaging agents. For this purpose, the HPLC profiles of the DNA adducts derived from incubation of the dihydrodiols with MCF-7 cells were compared to those obtained by treatment of the cells with the synthetic racemic series 2 diol epoxides of BcPh and 1,4-DFBcPh (Figure 4). From the HPLC profiles it was concluded that metabolically formed diol epoxides are the DNA-alkylating species, but that *in vivo* metabolic activation selectively produces only certain alkylation products. Although 1,4-DFBcPh is a model compound used for these structure–biology studies, its metabolic profile is consistent with that established for environmentally prevalent bay- and fjord-region PAHs.

Conclusions

In this paper we have described the extent of molecular distortion produced upon introduction of fluorine atoms into

the angular ring of BcPh and the ensuing effect on the metabolic activation to DNA-damaging metabolites. In this connection, X-ray crystallographic and computational analyses of related BcPh derivatives were undertaken. Surprisingly, 1,4-DFBcPh is just only slightly less nonplanar as compared to the corresponding dimethyl analogue 1,4-DMBcPh (33.5° versus 36.6°). However, P and M helicity that was observed in the case of 1,4-DMBcPh was not evident by NMR in the 1,4-DFBcPh derivatives. In those cases where crystallographic data were not obtained, computational analyses provide insight into the 3-dimensional structures. Strikingly, in solution the 1,4-DFBcPh series 1 (*syn*) diol epoxide exhibits a quasi-diaxial arrangement of hydroxyl groups that contrasts with the conformational preference of the corresponding BcPh diol epoxide wherein they are quasi-diequatorial. On the other hand, series 2 (*anti*) diol epoxides of both BcPh and 1,4-DFBcPh exhibit a quasi-diequatorial orientation of the hydroxyls. These results are borne out in the computational analyses as well. Also, a through-space F–H coupling is observed in each 1,4-DFBcPh derivative, and an analysis of the calculated and/or observed F–H bond distances as well as *J* values is provided. Finally, an assessment of the extent of DNA-damaging agents produced by metabolism and DNA alkylation was estimated using human MCF-7 cells. The results of this study show that increased molecular distortion may attenuate metabolic activation of PAHs, particularly the final P450-mediated oxidation of BcPh derivatives to DNA-alkylating diol epoxides. In this context, 1,4-DFBcPh dihydrodiol showed a ~4-fold-lower activation as compared to BcPh dihydrodiol, and prior results with the sterically congested 1,4-DMBcPh dihydrodiol had shown a ~11-fold-lower activation. Thus, a multifaceted approach involving synthesis, crystallography, computational, and biological studies has been utilized to provide insight into the structural influences of PAHs on their metabolic activation to DNA-damaging species. DNA

alkylation is ultimately linked to the tumorigenic and carcinogenic properties.

Experimental Section

For space considerations, synthetic details and some of the computational and X-ray crystallographic data are provided in the Supporting Information. Relevant details are provided below.

X-ray Analyses. Diffraction data were measured with Mo K α radiation (wavelength 0.71073 Å), with a rotating anode, a graphite monochromator, and an area detector. The rotation method with box integration was used. The program used for data collection and reduction was MADNES.²⁴ No absorption or extinction corrections were considered necessary ($\mu = 0.087$ for BcPh dihydrodiol). Data were refined by use of SHELX-97²⁵ and ICRFMLSQ.²⁶ The crystals used in this study were the result of several crystallization attempts.

Cell Culture and Treatment. The MCF-7 cells were grown in a 75 cm² flask in a 1:1 mixture of F-12 nutrient mixture and Dulbecco's modified Eagle's medium and 10% fetal bovine serum at 37 °C with 5% CO₂. The medium contained 15 mM HEPES buffer and sodium bicarbonate. The compounds were added to 80% confluent cells in 20 mL of fresh medium at a final concentration of 5 μ M (parent compounds), 1 μ M (dihydrodiols), or 0.25 μ M (diol epoxides). After 24 h, the cells were harvested by trypsin, washed in PBS, and kept at -80 °C until needed for DNA isolation.

DNA Isolation. MCF-7 cell pellets from two T 75 flasks per treatment were homogenized in lysis buffer (10 mM Tris, 1 mM Na₂EDTA, 1% SDS, pH 8). The homogenates were treated with RNase, DNase-free (50 U/mL), and RNase T1 (1000 U/mL) at 37 °C for 1 h, followed by treatment with proteinase K (500 μ g/mL) at 37 °C for 1 h. The DNA was extracted in light Phase Lock Gel tubes with equal volumes of Tris-equilibrated phenol and chloroform/isoamyl alcohol (24:1). The DNA was precipitated in ethanol. The DNA concentration was determined by UV absorbance at 260 nm.

³³P-Postlabeling of DNA Adducts. A 10 μ g sample of DNA isolated from MCF-7 cells after treatment was digested with nuclease P1 (0.4 U) and prostatic acid phosphatase (350 mU) and radiolabeled by T4 polynucleotide kinase (18 U) and [γ -³³P]ATP (5 μ Ci, 3000 Ci/mmol). The ³³P-labeled samples were digested with snake venom phosphodiesterase (15 mU) and apyrase (100 mU).²⁷

The postlabeled samples were cleaned to remove unbound ³³P

prior to HPLC analysis on a Sep-Pak C₁₈ cartridge and eluted in 2 mL of methanol and ammonium hydroxide (95:5). The radioactivity of the samples was determined by liquid scintillation counting, and 1 million counts were analyzed by HPLC. The amount of adducts was calculated on the basis of the postlabeling efficiency of (7*R*,8*S*,9*S*,10*R*)-7,8-dihydroxy-9,10-epoxy-7,8,9,10-tetrahydro[1,3-³H]benzo[*a*]pyrene.

HPLC Analysis. HPLC analysis was conducted on a C-18, 4.6 \times 250 mm, 5 μ m particle size column using an HPLC system equipped with an autosampler. The peaks were detected with a 400 μ L dry cell on an HPLC radioactive detector (a peak of 1 V contained 5000 disintegrations per minute). The HPLC method for benzo[*a*]pyrene, DMSO, and all diol epoxide samples utilized buffer A (0.05 M NH₄H₂PO₄ in water) and solvent B (methanol). The flow rate was 1 mL/min using a gradient from 44% to 55% B in 5 min, to 60% in 10 min, to 90% in 30 min, to 100% in 35 min, and to 44% in 40 min. For 1,4-DFBcPh and BcPh samples, solvent B was 50:50 methanol and acetonitrile and the gradient was 110 min long, from 37% to 38% B in 20 min, to 40% B in 40 min, to 43% in 60 min, to 49% in 80 min, and to 95% B in 110 min.

Acknowledgment. A portion of the synthetic work was performed by S.C. and M.K.L. at ChemSyn Laboratories under NIH (NCI) Contract 5N01 CB-061004. Mr. Joe Saugier (ChemSyn) is thanked for his assistance. M.K.L. and B.Z. were supported via NIH (NIGMS) Grant S06 GM008168-27, and NIH RCMI Grant G12 RR03060 provided infrastructural support at The City College of New York. B.Z. was also partially supported by NSF Grant CHE-0516557. J.P.G., H.L.C., and A.K.K. were supported by NIH (NCI) Grants 5R01 CA-010925 and CA-006927, K.L. and T.O. were supported by NIH (NCI) Grant 2R15 CA078235-02A1, and W.M.B. and T.J.M. were supported by NIH (NCI) 5R01 CA-028825.

Supporting Information Available: Synthetic details, computational results, GIAO NMR data, NICS values, crystal data for dihydrodiols of BcPh and 1,4-DFBcPh as well as diffraction measurements, two additional views of BcPh and 1,4-DFBcPh dihydrodiols determined by X-ray analysis, materials as well as their sources for the cell culture and ³³P postlabeling experiments, ¹H and ¹⁹F NMR spectra of **3–11**, CIF files for 1,4-DFBcPh, 1,4-DFBcPh dihydrodiol, and BcPh dihydrodiol, and PDB files for 1,4-DMBcPh, 1,4-DFBcPh, and the dihydrodiols of BcPh and 1,4-DFBcPh. This information is available free of charge via the Internet at <http://pubs.acs.org>.

JO071145S

(27) Ralston, S. L.; Lau, H. H.; Seidel, A.; Luch, A.; Platt, K. L.; Baird, W. M. *Cancer Res.* **1994**, *54*, 887–890.

(24) Pflugrath, J.; Messerschmidt, A. MADNES. Munich Area Detector (New EEC) System, version EEC 11/09/89, with enhancements by Enraf-Nonius Corp., Delft, The Netherlands, 1989.

(25) Sheldrick, G. M.; Schneier, T. R. *Methods Enzymol.* **1997**, *277*, 319–343.

(26) Carrell, H. L. ICRFMLS, modification of UCLALS4. Program from The Institute for Cancer Research, Fox Chase Cancer Center, Philadelphia, PA, 1975.